Elastic moduli and acoustic symmetry of ferroelastic $LaNbO_4$ and $BiVO_4$

1989 J. Phys.: Condens. Matter 1 2875

(http://iopscience.iop.org/0953-8984/1/17/009)

J. Phys.: Condens. Matter **1** (1989) 2875–2890. Printed in the UK

Elastic moduli and acoustic symmetry of ferroelastic $LaNbO_4$ and $BiVO_4$

E S Fisher
Materials Consulting Services, 2923 Cedar Knoll Court, Minnetonka, MN 55343, USA

Received 28 June 1988, in final form 30 October 1988

Abstract. The single-crystal elastic moduli for the monoclinic (ferroelastic) phases of $BiVO_4$ and $LaNbO_4$ at 300 K are analysed with respect to variations of elastic properties in directions normal to the axes of twofold symmetry. In both crystals the directions of minimum shear modulus, $G = 1/S'_{55}$, are within 4° of rotation from the directions of the ferroelastic domain walls. This minimum G-value in $LaNbO_4$ is at least one order of magnitude smaller than in $BiVO_4$. The maxima in G occur in directions rotated 45° to the domain-wall directions and are therefore parallel to the principal axes of the spontaneous strain at the phase transition from the high-temperature paraelastic tetragonal II phase. In contrast, the Young's moduli have maximum values parallel to the domain-wall directions but minimum values parallel to the axes of spontaneous strain. Thus tensile strains for a given tensile stress are maximised in these directions. However, the cross-coupling compliance moduli, S'_{15} and S'_{35}, both have zero values for these principal axes of the spontaneous strain. Therefore the elastic tensile strains produce no accompanying shear strains. The elastic symmetry in domain-wall directions within the plane normal to the twofold symmetry axes is almost identical to that for the tetragonal II prototype phase. Thus, when the Cartesian reference axes are chosen as those directions where $C'_{16} = 0$ in the tetragonal scheelite phase the number of C'_{ij} and S'_{ij} in the monoclinic phase are reduced to near correspondence to tetragonal symmetry. These are the only directions in the monoclinic crystal where the symmetry of the prototype is preserved.

1. Introduction

$BiVO_4$ and $LaNbO_4$ are two prominent examples of monoclinic ferroelastic phases produced by acoustic-mode softening from a scheelite ($CaWO_4$) type of crystal stucture. In their paraelastic phase the crystals have 4/m tetragonal II Laue symmetry. As with all tetragonal crystals, the elastic moduli are referred to Cartesian XYZ axes in which the Z axis has four-fold rotation symmetry and the X and Y axes lie in the tetragonal tetragonal (001) plane and are parallel to the a and b lattice directions. The tetragonal II structure differs from the tetragonal I in that the a and b axes are not axes of two-fold symmetry. Therefore, with respect to the conventional a and b axes the matrix of principal elastic stiffness moduli contains seven non-zero C_{ij} in contrast to six C_{ij} for tetragonal I. The seventh independent modulus is C_{16}, which allows for a shearing of (010) planes produced by a tensile strain parallel to [100]. The presence of this extra modulus and the absence of two-fold symmetry are the result of the setting angle of

0953-8984/89/172875 + 16 $02.50

the W—O bonds in the tungstate tetrahedra being non-parallel to the ⟨100⟩ or ⟨010⟩ directions, as noted in Zalkin and Templeton (1964) and Farley *et al* (1975).

The absence of the twofold symmetry along the *a* and *b* axes produces two interesting but complicating aspects to the elastic and/or acoustic properties of scheelite crystals. The major factor of interest to the transformation to the ferroelastic monoclinic phase is that there does exist a set of X' and Y' axes, offset from the conventional X and Y axes, that do in fact have twofold acoustic symmetry by virtue of the disappearance of the cross-coupling modulus, C'_{16}. Thus by rotating the X' and Y' axes by an angle θ_0 from X and Y the new, or primed, elastic modulus matrix has only the six C_{ij}, namely C'_{11}, C'_{33}, C'_{13}, C'_{44}, C'_{66} and C'_{12}. These unique axes of acoustic symmetry have the conventional property that they are directions of pure acoustic-mode propagation, where the atomic displacement directions are parallel to the wave propagation direction for a longitudinal acoustic mode and 90° to the wave propagation direction for each of the two transverse acoustic modes. It is precisely the pure C'_{66} mode in $BiVO_4$ propagated in either of the two acoustic symmetry directions that decreases with decreasing temperature in the paraelastic structure above 528 K and becomes very near zero value at $T_c = 528$ K (Tokumoto and Unoki 1983). It is this mode softening that produces the spontaneous strain in the $BiVO_4$ crystal at T_c, the tetragonal → monoclinic phase transition temperature, as shown by David (1983). And this spontaneous strain, produced by the two mutually perpendicular pure transverse modes, creates the monoclinic distortion within the ferroelastic domains and the directions in the domain wall that are free of distortion and transform as the symmetric representation of the paraelastic tetragonal II phase (David and Wood 1983). It is this strong relationship between the acoustic modes in the paraelastic phase and the monoclinic distortion that makes a study of the elastic properties in the ferroelastic phase of prime interest.

The other complicating factor produced by the absence of the twofold elastic symmetry about the crystallographic *a* and *b* axes of the tetragonal phase is in the experimental technique of propagating ultrasonic waves in single crystals. In wave propagation within anisotropic media the particle displacements are in general not pure modes. Consequently, the directions of displacement are neither parallel nor perpendicular to the normal to the wave front and the three normal modes for a given direction of propagation are resolved into quasi-longitudinal and quasi-transverse. Similarly, the kinetic and potential energy flux associated with the wave front is in general not parallel to the direction of wave propagation. Consequently, the maximum acoustic energy will travel at an angle to the wave front and will contact the echo-reflecting surface at positions that may not be detected by a sensor that covers only part of the reflecting face. This problem will of course not be present in a geometry where the sensor is the same as the original wave-producing piezo-electric transducer which is designed to detect echoes, since the energy flux retraces its path after reflection from a pair of parallel planes. However, if the energy flux deviates widely from the propagation direction and the crystal sample is small in dimensions, the energy flux could reflect at a non-parallel face and mode-convert to produce spurious wave modes that do not correspond to that intended. In these cases the measured time lapse for total travel time will be incorrect, perhaps by very large deviations from the correct values. This phenomenon has been studied in scheelite crystals in a series of papers and by Farley and co-workers (Farley and Saunders 1972, Farley *et al* 1973, 1975) and the energy flux deviations for shear (transverse) modes in molybdates and tungstates have been found to be as large as ±45°. This factor could be of even greater importance in the case of monoclinic symmetry with the addition of domain walls in very small crystals. Consequently, although the

measurements of the acoustic velocities in these small samples of ferroelastic phases are precise, the data may not represent the intended acoustic mode.

This paper is primarily an interpretation of the results of an experimental investigation of the single-crystal elastic moduli of monoclinic $LaNbO_4$ at 300 ± 2 K, which were reported by Nevitt *et al* (1986). The latter paper described the details of the measurements of the 13 elastic stiffness moduli, C_{ij}, using an interferrometric ultrasonic technique that provides precise measurements of acoustic wave velocities. The method of data treatment and some discussion of error sources are summarised in § 3.1 of this paper, where it is noted that the internal consistency of the wave velocity measurements for the 21 different acoustic modes involved in this study was not completely in accord with numerical relations dictated by the Christoffel equations. Nevertheless, a set of 13 C_{ij} were determined by an iteration of the C_{ij} values to provide the least-mean-square deviations from the Christoffel relations. The mean-square deviation was of the order of 1%.

The major purpose of the present paper is to confirm some of the details of the existing models for the tetragonal-to-monoclinic phase transition, which are now based almost totally on the C_{ij} of the tetragonal II phase. We do this by calculating how the C_{ij} vary as the Cartesian coordinate axes are rotated about the monoclinic two-fold axis. This approach reveals several features of the elastic properties of the ferroelastic phase that were previously not recognised. It also provides a firm basis for depicting the similarity between the elastic symmetry of the domain walls in the ferroelastic phase to that of the paraelastic tetragonal phase. In order to relate the new, primed, axes to the physical monoclinic crystal, the conventions for the unprimed axes and their relations to the tensor notations used in tetragonal crystals are described in § 2.1.

Because the preponderance of past work on this tetragonal-to-monoclinic transition has been focused on the $BiVO_4$ crystal and its properties, we continue § 2 to cite briefly the relevant studies that have been carried out for $BiVO_4$ so that we can properly interpret the $LaNbO_4$ data. In presenting this $BiVO_4$ review, we add to the literature on this important prototype ferroelastic by showing that the elastic symmetry as calculated from the C_{ij} for monoclinic $BiVO_4$ (Avakyants *et al* 1982) does in fact correspond well to predictions based on Brillouin scattering work and on the extensive studies of the spontaneous strain by David (1983) and David and Wood (1983). Avakyants *et al* used an experimental technique and a least-squares fit to Christoffel equations that were very similar to those used for the $LaNbO_4$ study (Nevitt *et al* 1986). Section 2.2 reviews what is known of the relation of the soft acoustic mode to domain-wall orientation from studies of the tetragonal phase of $BiVO_4$ and §§ 2.3 and 2.4 extend the review to the monoclinic phase.

Section 3 includes a brief review of the experimental results for $LaNbO_4$ and the analysis of the elastic properties and symmetry for $LaNbO_4$ at 300 K. Section 4 is the summary, with emphasis on the applications to $LaNbO_4$. The principal conclusions are related to the variations of the elastic properties within the basal planes, (010), of $LaNbO_4$ and monoclinic ferroelastic crystals in general. As was previously shown by Nevitt *et al* (1986), the directions defined by the intersections of the domain walls and the basal plane are minimum-shear-modulus directions. In addition, the domain-boundary directions have the maximum Young's modulus and the principal axes of the spontaneous strain, at 45° to the domain walls, are directions of minimum Young's modulus. A third point of interest is the variation at 300 K of the elastic symmetry from pseudo-tetragonal at domain boundaries to maximum monoclinic symmetry at the principal axes of the spontaneous strain tensor.

2. Background

2.1. Conventions for C_{ij}

Except for the work of Avakyants *et al* (1982), to be discussed here, and Nevitt *et al* (1986), the elastic modulus measurements for $BiVO_4$ and $LaNbO_4$ have previously been carried out in the paraelastic tetragonal phase using Brillouin light scattering techniques. Consequently the elastic constant matrix (figure 1(*a*)) is based on the standard crystallographic convention where the fourfold axis of symmetry is noted as the $c = Z$ axis and the XY plane is the mirror plane, also indicated in figure 1(*a*). The standard crystallographic convention for monoclinic symmetry (figure 1(*b*)) uses the $b = Y$ axis as the axis of symmetry and the XZ plane as the mirror plane. Consequently, in relating the elastic moduli of the monoclinic phase with the equivalent physical directions in the parent tetragonal phase, it is necessary to interchange the tensor subscript numbers 2 and 5 in the monoclinic phase with the numbers 3 and 6, respectively, in the parent phase. Thus, because of this interchange, the modulus C_{16} in the tetragonal phase becomes the modulus C_{15} in monoclinic symmetry, for example, and because of the decrease in crystal symmetry the monoclinic matrix has 13 non-zero entries with respect to the standard XYZ coordinates, whereas tetragonal II has seven non-zero moduli. For the convenience of the reader, table 1 gives the pairing of physically related moduli.

2.2. Measurements of the soft acoustic phonon mode and domain-wall orientations in tetragonal $BiVO_4$

From the results of David (1983), David and Wood (1983), Tokumoto and Unoki (1983), Cho *et al* (1982) and Benyuan *et al* (1981) it is established that the soft transverse acoustic mode for waves propagating in the (001) tetragonal plane of $BiVO_4$ occurs for θ_0, the

Tetragonal II

$$\begin{vmatrix} C_{11} & C_{12} & C_{13} & 0 & 0 & C_{16} \\ C_{12} & C_{11} & C_{13} & 0 & 0 & C_{16} \\ C_{13} & C_{13} & C_{33} & 0 & 0 & 0 \\ 0 & 0 & 0 & C_{44} & 0 & 0 \\ 0 & 0 & 0 & 0 & C_{44} & 0 \\ C_{16} & C_{16} & 0 & 0 & 0 & C_{66} \end{vmatrix}$$

Monoclinic

$$\begin{vmatrix} C_{11} & C_{12} & C_{13} & 0 & C_{15} & 0 \\ C_{12} & C_{22} & C_{23} & 0 & C_{25} & 0 \\ C_{13} & C_{23} & C_{33} & 0 & C_{35} & 0 \\ 0 & 0 & 0 & C_{44} & 0 & C_{46} \\ C_{15} & C_{25} & C_{35} & 0 & C_{55} & 0 \\ 0 & 0 & 0 & C_{46} & 0 & C_{66} \end{vmatrix}$$

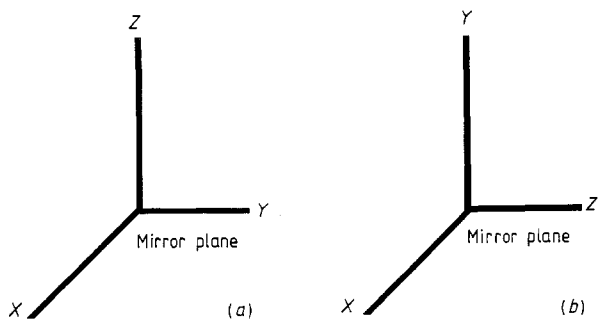

Figure 1. Matrix of elastic stiffness moduli for tetragonal II and for monoclinic symmetry.

Table 1. Interchange of modulus subscripts between conventional monoclinic and tetragonal II symmetry.

Monoclinic modulus (13 total)	Tetragonal II modulus (7 total)
C_{11}	C_{11}
C_{12}	C_{13}
C_{13}	C_{12}
C_{15}	C_{16}
C_{22}	C_{33}
C_{23}	C_{13}
C_{25}	0
C_{33}	C_{11}
C_{35}	C_{16}
C_{44}	C_{44}
C_{46}	0
C_{55}	C_{66}
C_{66}	C_{44}

angle between the wave propagation direction and the ⟨100⟩ direction, in the range of $35 \pm 3°$ and at $125 \pm 3°$. It is also well established that these directions correspond to domain-wall directions in the ferroelastic phase at or just below $T_c \equiv 528$ K. David and Wood (1983) have measured the domain-wall orientation in the monoclinic phase at 300 K and report the value of 54.1° from the '$+a$' axis of the unit cell, which is, in turn, 89.6° from the $+c$ axis. This is in essential agreement with the θ_0 value of 35° noted above assuming that the referenced axes are at complementary angles.

The direct linear correspondence between the direction of the soft acoustic mode, the domain-wall orientation and the acoustic symmetry direction of the tetragonal phase in $BiVO_4$ has not been verified or confirmed because of the absence of direct measurements of the elastic moduli above T_c. To do this it will be necessary to evaluate the appropriate C_{ij} values with reference to the standard reference axes, X, Y and Z, and then calculate the values of the new sets of C_{ij}, noted as C'_{ij}, with reference to the new set of Cartesian axes, X', Y' and Z'. This is done by performing the similarity transformation

$$\mathbf{C}' = \boldsymbol{\alpha}\mathbf{C}\boldsymbol{\alpha}^{-1} \tag{1}$$

where $\mathbf{C}$ is the matrix of C_{ij} with reference to the standard axes (see figure 1) and $\boldsymbol{\alpha}$ is a 6×6 matrix of direction cosines relating the primed and standard sets of X, Y and Z axes. Since the change involves only a rotation about the standard tetragonal Z axis, the equations for the C'_{ij} in terms of the C_{ij} are considerably simpler than in the general case. The modulus of interest with regard to the direction of pure mode propagation in the (001) is C'_{16}, which must disappear at the critical angle, θ_0. The equation of interest to determine θ_0 is

$$C'_{16} = 0 = C_{16}\cos(4\theta_0) - \tfrac{1}{4}(C_{11} - C_{12} - 2C_{66})\sin(4\theta_0). \tag{2}$$

2.3. Soft acoustic modes and acoustic symmetry axes in monoclinic $BiVO_4$

Tokumoto and Unoki (1983) have made direct measurements of Brillouin frequencies as a function of longitudinal and transverse wave propagation direction in the (010)

plane of the monoclinic ferroelastic phase at temperatures of 297, 396 and 461 K. It should be emphasised here that the normal to the (010) plane is parallel to the fourfold Z axis of the tetragonal phase. Although the results are complicated by the presence of at least two domains producing duplicate results, their data show that the transverse shear modes with displacements in the (010) plane have maximum and minimum velocities at propagation directions corresponding to the acoustic symmetry angles of the tetragonal phase. Their given data are, however, not sufficiently quantitative to be of value in comparing the angles of the soft mode directions among the paraelastic and ferroelastic phases.

Avakyants *et al* (1982) have determined the 13 elastic moduli in monoclinic $BiVO_4$ at room temperature from measurements of acoustic wave velocities by pulse–echo ultrasonics, by the Schaeffer–Bergman light diffraction interference technique and by Brillouin scattering. Their paper gives only the measured ultrasonics ρV^2 values for each of their 16 wave modes and selected only those ρV^2 (ρ = density, V = wave velocity) that were confirmed by the other two techniques for determining the best-fit values of the C_{ij} with reference to an XYZ Cartesian coordinate system that is based on the standard monoclinic crystallographic axes. The C_{ij} values are given in table 2. The probable errors are given as 1% to 'somewhat greater'. The first six C_{ij} listed are those that reflect the values of ρV_L^2 (longitudinal stiffness) and ρT_T^2 (transverse stiffness) in the (010) plane and also the acoustic symmetry or C'_{ij} values in the (010) plane.

The variations of ρV_L^2 and ρV_T^2 with propagation direction in the (010) plane are plotted in figure 2, as evaluated from the standard C_{ij} and the solutions of the secular determinant

$$\begin{vmatrix} (\Gamma_{11} - \rho V^2) & 0 & \Gamma_{13} \\ 0 & (\Gamma_{22} - \rho V^2) & 0 \\ \Gamma_{13} & 0 & (\Gamma_{33} - \rho V^2) \end{vmatrix} = 0 \tag{3}$$

Table 2. Elastic stiffness moduli and some compliance moduli S_{ij} of monoclinic $BiVO_4$ (Avakyants *et al* 1982) and $LaNbO_4$ (Nevitt *et al* 1986) at 300 ± 2 K, in units of 10^2 GPa for C_{ij} and $(10^2\ \text{GPa})^{-1}$ for S_{ij}, for Z axis parallel to 'C' lattice direction.

Modulus	$BiVO_4$	$LaNbO_4$
C_{11}	1.045 (S_{11} = 1.471)	2.42 (S_{11} = 6.469)
C_{33}	1.638 (S_{33} = 1.002)	2.12 (S_{33} = 14.181)
C_{55}	0.600 (S_{55} = 2.043)	0.118 (S_{55} = 102.8)
C_{13}	0.620 (S_{13} = −0.620)	1.85 (S_{13} = 9.177)
C_{15}	−0.227 (S_{15} = 0.695)	0.041 (S_{15} = 22.814)
C_{35}	0.132 (S_{35} = −0.477)	0.293 (S_{35} = −36.2)
C_{22}	1.103	1.77
C_{12}	0.222	0.838
C_{66}	0.364	0.536
C_{44}	0.393	0.439
C_{23}	0.527	0.498
C_{46}	0.014	−0.089
C_{25}	−0.035	−0.164
$(C_{11} - C_{13})/2$	0.213	0.285
$(C_{33} - C_{13})/2$	0.509	0.135

where the Γ_{ij} are the Christoffel equations given, for example, by Cady (1946). Of the three roots to this set of equations we are only concerned here with the two roots involved in the binary equation. The third root is that for the pure transverse mode with displacement along the twofold Y axis.

For ρV_L^2 the rotation symmetry is far from the fourfold symmetry found in the tetragonal phase and the minima and maxima values occur at rotation angles that are not related to the domain-boundary positions in the (010) plane. The symmetry in transverse moduli, ρV_T^2, is, however, closely related to the tetragonal acoustic symmetry and to the angle of the domain walls in the monoclinic phase as measured by David and Wood (1983). As shown in figure 2, the C_{ij} values of Avakyants *et al* (1982) give the minimum ρV_T^2 values at 54 ± 1° from the monoclinic a axis and 153° or 63° from the c axis. The error noted here indicates that ρV_T^2 values were the same at 53, 54 and 55°. It should be noted that these minima are separated by 99°, as opposed to the 90° symmetry of the acoustic symmetry axis in the tetragonal phase. The 54° value is, however, almost identical to domain-boundary orientation measured by David and Wood. The deviation of 9° from the tetragonal axis or from the ferroelastic domain walls at 527 K is about 8° more than predicted from the lattice constant measurements (David 1983).

2.4. *Rotated axial symmetry and C'_{ij} in $BiVO_4$*

The purpose of calculating the elastic stiffness moduli relative to a rotation of the X and Z Cartesian axes in the (010) plane of the ferroelastic monoclinic crystal is to confirm the concept that the crystal structure at the domain boundary contains those directions that transform with the same symmetry as in the tetragonal II prototype. Since the tetragonal symmetry is fourfold the elastic, or acoustic, symmetry when the X' and Z' axes are in the domain walls should be very close to that for the $4/m$ acoustic symmetry, i.e. six C_{ij} instead of 13 C_{ij}. The results obtained by starting with the C_{ij} (Avakyants *et al* 1982) and applying the similarity transformations of equation (1) are given in figures 3–5. The longitudinal moduli C'_{11} and C'_{33} vary with the rotation angle θ in the same way as ρV_L^2, with a 90° phase difference between C'_{11} and C'_{33} (figure 3). The variation of

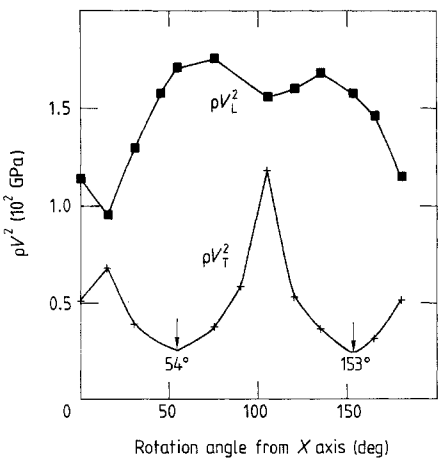

Figure 2. Variation of ρV_L^2 and ρV_T^2 in (010) plane with rotation from X to $-X$ axes for $BiVO_4$.

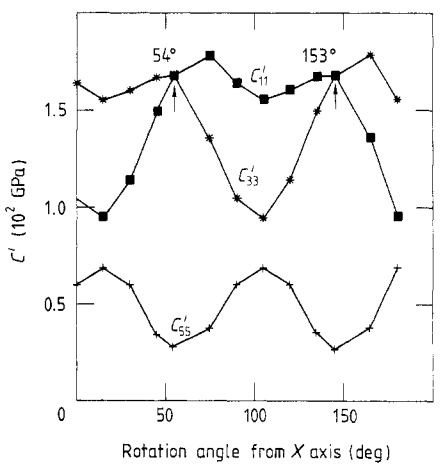

Figure 3. Values of C'_{11}, C'_{33} and C'_{55} for $BiVO_4$ as a function of rotated X' and Z' axes about Y axis.

C'_{55} with θ is also very similar to the ρV_T^2 rotation in figure 2. The minimum values occur, however, at 58 ± 1° and 148 ± 1°, in contrast to the 54 and 153° for ρV_T^2. The maximum C'_{55} occurs at $X' = 13 \pm 1°$ and 103 ± 1°, which corresponds to the principal axes for the transformation strain.

Figures 4 and 5 show the variation of the compliance moduli, S'_{ij}, which are calculated as the inverse matrix entries from the C'_{ij} given in figure 1. In contrast to the C'_{ij} the variations of S'_{11}, S'_{33} and S'_{55} are very close to having the 90° repetition of fourfold symmetry. As in the case of C'_{11} and C'_{33} they have the $S'_{11} = S'_{33}$ condition near the domain-wall directions, $X' = 58°$, and S'_{55} has its maximum (weakest) value at the same θ-value. It should be noted here that the compliance moduli, S'_{ij}, have inverse force units and are also more useful than C'_{ij} in directly calculating strains proposed by a given stress vector. Therefore, the Young's moduli ($1/S'_{11}$ or $1/S'_{33}$) along the domain-wall directions are equal and at their maximum values, whereas at the principal axes of the spontaneous strain, i.e. $X' = 14$ and 104°, Young's moduli are at their minimum values and also at maximum derivation from the pseudo-tetragonal symmetry. The shear modulus for distorting the basal XZ plane, $1/S'_{55}$, is, however, strongest in the principal strain axes directions. Figure 5 shows the variation of S'_{15} and S'_{35} with X' rotation. Both moduli couple shear strains to tensile or compressive stress in the following equation:

$$e_{13} = S'_{15}\sigma'_X + S'_{35}\sigma'_Z \tag{4}$$

where e_{13} is the (010) plane shear related to the rotated X' and Z' axes and σ is the tensile or compressive stress component. For $BiVO_4$ $S'_{35} = S'_{15} \simeq 0$ at X' along the principal axis of spontaneous strain and $S'_{35} = S'_{15} \neq 0$ at the domain-boundary direction. Thus, for a tensile or compressional stress along either of the orthogonal principal strain axes, there is no induced shear strain.

The net effect of the rotation of X' and Z' to the domain-boundary directions is to reduce the number of non-zero independent C'_{ij} (or S'_{ij}) to 10, as listed in table 3. This is basically due to the equivalence of the X' and Z' directions. The non-equivalence gradually increases as X' and Z' are rotated to the principle axes of spontaneous strain

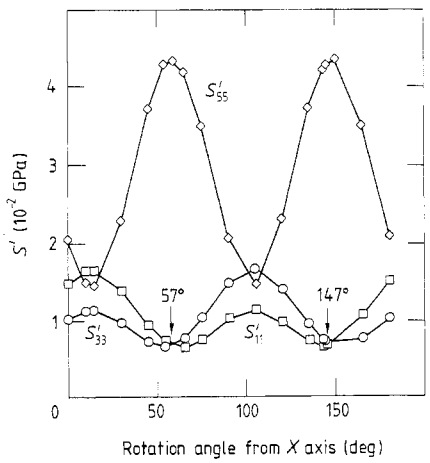

Figure 4. Variation of compliance moduli S'_{11}, S'_{33} and S'_{55} for $BiVO_4$ with rotation of X' and Z' axes about Y.

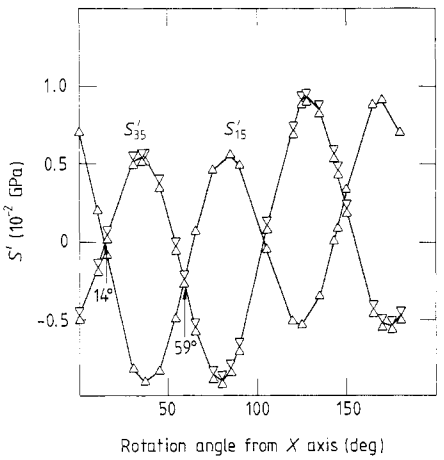

Figure 5. Variation of S'_{15} and S'_{35} for $BiVO_4$ with rotation of X' and Z' axes about Y.

Table 3. C'_{ij} for $BiVO_4$ with X' and Z' domain-wall direction in (010) plane, $X' = 54°$ from 'a' direction.

	Corresponding C_{ij} in tetragonal phase
$C'_{11} = C'_{33} = 1.674$	C'_{11}
$C'_{55} = 0.265$	C'_{66}
$C'_{13} = 0.280$	C'_{12}
$C'_{15} = C'_{35} = 0.15$	$C'_{16} = 0$
$C'_{22} = C'_{22} = 1.103$	C_{33}
$C'_{12} = C'_{23} \times 0.375$	C_{13}
$C'_{46} = 0.0020$	0
$C'_{25} = 0.15$ (maximum)	0
$C'_{44} = 0.360$	C_{44}
$C'_{66} = 0.397$	C_{44}

and $(S'_{11} - S'_{33})$ becomes a maximum. The more unexpected result is that the cross coupling between extensional strains and shear stress, S'_{15} and S'_{35}, disappears. This result is the physical analogue to the analysis of David (1983), which gives the result that the ferroelastic phase is the most stable with respect to external tensile or compressive stress when the latter is collinear with the axes of the spontaneous strain tensor.

3. Elastic moduli and acoustic symmetry in ferroelastic $LaNbO_4$

3.1. Determination of the elastic moduli

A brief report on the experimental work and results of an extensive study of acoustic wave velocities in single-crystal $LaNbO_4$ is presented in Nevitt *et al* (1986). The C_{ij} given there were from data obtained from a phase-comparison ultrasonic interferometer method and from Brillouin scattering. The errors in ultrasonic wave velocity measurements are of the order of 0.05–0.10% in error. For high-symmetry crystals the estimated errors in C_{ij} would then be of the order of 0.10–0.20% maximum, and these estimates are readily confirmed by performing redundant measurements so as to evaluate internal consistency. This straightforward procedure, using velocity measurements for 23 different wave modes and the appropriate Christoffel equations, did not produce the expected confirmation of the values of the 13 C_{ij} in monoclinic $LaNbO_4$ crystals. The present author believes that the prime reason for the difficulties in obtaining proper internal consistency is most probably related to the wide deviations in ultrasonic energy flux from the propagation directions, as discussed in the introduction to this paper. The errors are probably the result of mode conversion occurring in one or more of the crystals with thickness dimensions of the order of 5 mm, but lateral dimensions of the order of 3 mm. Thus the wave energy maximum could readily travel at 45° to the thickness in these low-symmetry crystals and diffract from the side faces to give echo patterns that produce erroneous velocities. Nevertheless, the data that were obtained by the ultrasonic technique were generally consistent with Brillouin scattering data, with a significant difference occurring in only one shear mode. The ultrasonic data (to be published) and corresponding crystal orientations of the propagation and polarisation directions are given in table 4.

Table 4. Stiffness moduli, ρV^2, as calculated from the measured wave velocities, V, for 21 different wave modes in $LaNbO_4$.

V no.	Direction of wave propagation	Direction of displacement polarisation	ρV^2 (10^2 GPa)
1	⟨010⟩ = Y axis	⟨010⟩	1.770
2	⟨010⟩	Quasi-shear Z axis	0.589
3	⟨010⟩	Quasi-shear X axis	0.386
4	Normal to (−101)	⟨010⟩	0.569
5	Normal to (−101)	Quasi-long	2.511
6	Normal to (−101)	Quasi-shear	0.121
7	Normal to (101)	⟨010⟩	0.402
8	Normal to (101)	Quasi-long	2.053
9	Normal to (101)	Quasi-shear	0.206
10	Normal to (−101) = X axis	Quasi-long	2.437
11	Normal to (−100)	Quasi-shear in (010)	0.097
12	Normal to (−100)	⟨010⟩	0.548
13	Normal to (101) = Z axis	Quasi-long	2.094
14	Normal to (001)	⟨010⟩	0.431
15	Normal to (001)	Quasi-shear	0.163
16	45° to ⟨010⟩, 90° to ⟨001⟩	Quasi-long	1.832
17	Same as above	Quasi-shear in (001)	0.436
18	Same as above	⟨001⟩	0.582
19	45° to ⟨010⟩, 90° to ⟨100⟩	Quasi-long	1.740
20	Same as above	Quasi-shear in (100)	0.432
21	Same as above	⟨100⟩	0.607

The crystallographic directions and planes noted in table 4 are given with reference to the standard lattice directions for monoclinic $LaNbO_4$ where the angle β between the ⟨100⟩ and ⟨001⟩ directions is 94°. The ultrasonic wave propagation directions in the (010) plane were, however, selected with reference to the directions normal to the principal planes, which are not collinear with either the 'a' or 'c' directions. The elastic stiffness moduli, C_{ij}, were then calculated from a reference Cartesian coordinate system where the Y axis is the long axis of twofold symmetry and the X and Z axes are related to the crystallographic a and c directions as shown in figure 6. The values for the C_{ij} obtained by a non-linear least-squares fit of ρV^2 values to the Christoffel equations are given in Nevitt *et al* (1986) and also in table 2. The mean-square deviation was approximately 1% and a maximum probable error of 1% in each C_{ij} and 2% in each S_{ij} is assumed.

3.2. Rotated axial symmetry and C'_{ij} in $LaNbO_4$ at 300 K

The history of research on the soft acoustic mode at this transformation temperature, $T_0 \approx 770$ K, is similar to that for $BiVO_4$. Hara *et al* (1985) have measured the angular dependence of Brillouin scattering frequency shifts in the tetragonal phase at several temperatures including T_0 and have determined that the soft transverse acoustic mode occurs for the quasi-transverse mode propagated at 20° to the tetragonal ⟨100⟩ or ⟨010⟩ axes. At room temperature in the monoclinic phase Tsunekawa and Takei (1978) have identified the domain walls as the (602) and (20$\bar{6}$) planes, which would correspond to an angle θ_0 of 23 and 113° between the $+a$ axis and domain walls. Thus, it appears that the domain-wall orientations and soft-mode orientations are collinear and also are

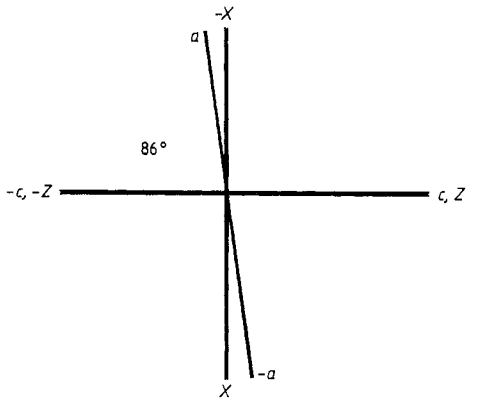

Figure 6. Orientation of adopted standard *XYZ* system relative to crystallographic *a*, *b* and *c* lattice directions in $LaNbO_4$. The *Y* axis and *b* direction are normal to plane of paper.

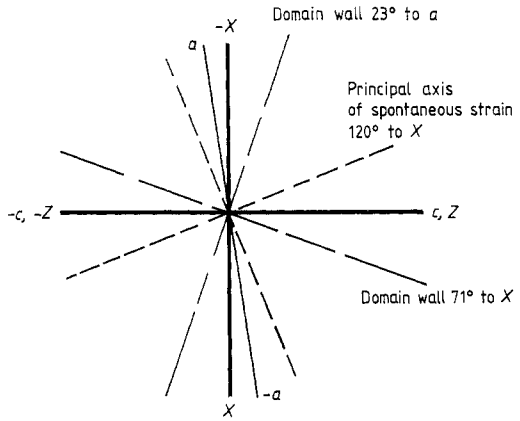

Figure 7. Orientation in (010) plane of domain walls and principal axes of spontaneous strain relative to *a* and *c* directions and adopted *X* axis for $LaNbO_4$.

relatively independent of temperature. This would place the domain walls at 71 and 161° from our *X* axis as noted in figure 7.

Figure 8 is the plot of ρV_L^2 and ρV_T^2 in the (010) plane of $LaNbO_4$ as a function of the angle θ rotation about the ⟨010⟩ direction. The two plots have similar character to those of figure 2 for $BiVO_4$. The ρV_T^2 plot has pseudo-tetragonal symmetry, whereas the ρV_L^2 variation lacks the approach to four-fold symmetry. However, the ρV_T^2 curve shows much more pronounced maxima and minima than in $BiVO_4$. The maximum-to-minimum ratio for $LaNbO_4$ is about 20, compared with about 3 for $BiVO_4$. In fact the minimum ρV_T^2 is very close to zero if the probable errors are taken into account. Another difference between $BiVO_4$ and $LaNbO_4$ is that the θ for both maxima and minima for the latter appear to be close to the 90° apart as expected from the relationship to the acoustic symmetry axes in the paraelastic phase. The minima θ angles of 75 and 165° correspond well with the (602) plane domain wall found by Tsunekawa and Takei (1978) as indicated in figure 7.

The elastic symmetry derived from rotating the X' and Z' axes from the adopted standard *X* and *Z* axes are also as expected from the $BiVO_4$ results. Figure 9 shows the variations of C'_{11} and C'_{33}, which are both similar to the ρV_L^2 plots. They cross at $\theta = 78$ and 168°, with possible errors of 1.5°, or $C'_{11} = C'_{33}$ at 1.5 to 4.5° beyond the domain walls. The compliance moduli, S'_{11} and S'_{33} (figure 10), are, however, very near the tetragonal symmetry and $S'_{11} = S'_{33}$ at $75 \pm 2°$, which is the same θ angle as the minimum ρV_L^2 and C'_{55} shear moduli and the maximum S'_{55} shown in figure 11. At the domain boundaries the magnitude of S'_{55} is a factor of 32 greater than the maximum S'_{55} in $BiVO_4$. This ratio converts directly to the ratio of e_{13} strain magnitudes produced by a given σ_{13} stress. These large differences between $LaNbO_4$ and $BiVO_4$ also exist in the S'_{33} and S'_{11} magnitudes at $\theta = 30$ and 120° which correspond to the principal axes of the spontaneous transformation strain. The tensile strain response to a tensile stress along these two axes is 32 times greater in $LaNbO_4$.

As in $BiVO_4$, the rotated S'_{35} and S'_{15} values (figure 12) which relate the tensile or compressional stresses along the principal axes of spontaneous strain to a shear strain distorting (010) plane are pecisely equal and zero, $S'_{15} = S'_{35} = 0$ at $\theta = 30$ or 120°. Thus

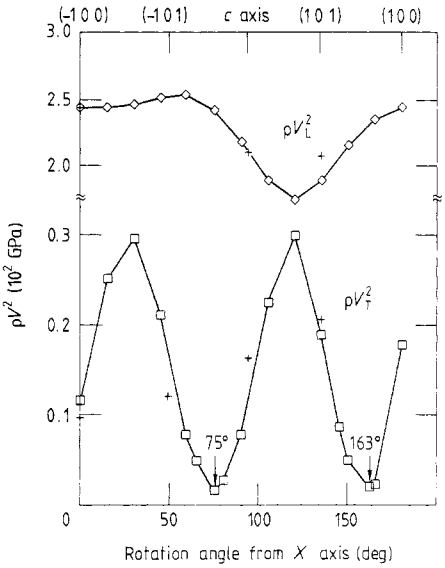

Figure 8. Variation of ρV_L^2 and ρV_T^2 in (010) plane of $LaNbO_4$ with rotation from standard adopted X axis. Crosses (+) are measured data points.

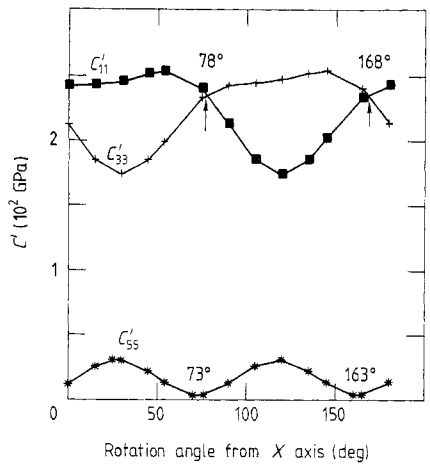

Figure 9. Variations in C'_{11}, C'_{33} and C'_{55} with rotation of X' and Z' axes in (010) plane in $LaNbO_4$.

the conclusions of David (1983) from free-energy considerations are again valid, i.e. the ferroelastic phase is most stable with respect to external tensile stress when the latter is parallel to the principal axes of spontaneous strain.

The elastic symmetry for X' at 75 and 165° to X, in the (010) plane, is again increased significantly, as in $BiVO_4$. The reduction from 13 to 10 independent C'_{ij} comes about because $C'_{11} = C'_{33}$, $C'_{15} = C'_{35}$ and $C'_{44} = C'_{66}$ (figure 13). The values of the C'_{ij}, the Young's moduli $E_{X'} = E_Z$ and the shear modulus $G_{X'Z'}$ with X' in the domain wall are

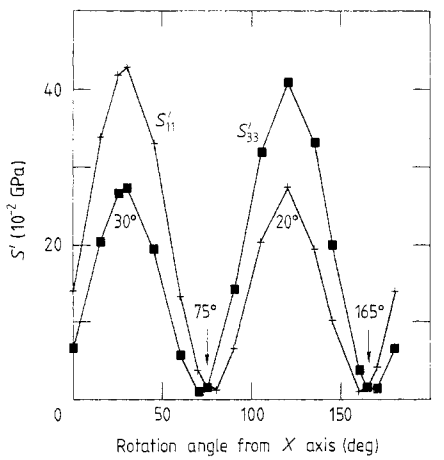

Figure 10. Variation of compliance moduli S'_{11} and S'_{33} with rotation of X' and Z' axes in (010) plane of $LaNbO_4$.

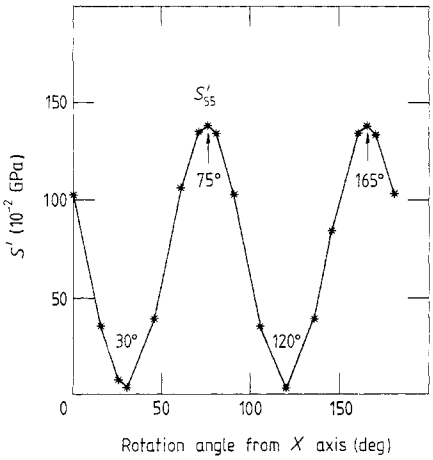

Figure 11. Variation of shear compliance modulus S'_{55} with rotation of X' and Z' axes in (010) plane of $LaNbO_4$.

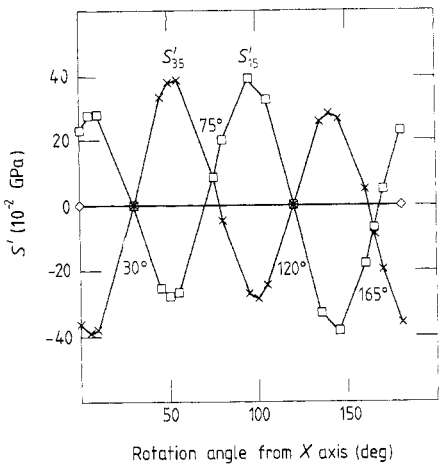

Figure 12. Variation of S'_{15} and S'_{35} with rotation of X' and Z' axes in (010) plane of $LaNbO_4$.

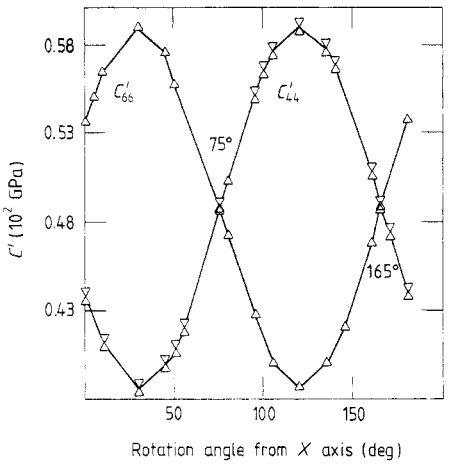

Figure 13. Variation of C'_{66} and C'_{44} with rotation of X' and Y' axes in (010) plane of $LaNbO_4$.

given in table 5. It should be noted that $G_{X'Z'}$ is considerably smaller than C'_{55} at this rotation because the S'_{55} value reflects the compliance through S'_{15} and S'_{35} of the extensional strains e'_{11} and e'_{33} when a σ'_{13} shear stress is applied to the crystal. The C'_{55} modulus reflects the same shear strain, e'_{13}, when the e'_{11} and e'_{33} are constrained.

As in $BiVO_4$. the difference between C'_{11} and C'_{33} and between C'_{44} and C'_{66} is maximised when the X' and Z' axes are parallel to the principal axes of the spontaneous strain. Because $C'_{15} = C'_{35} = 0$ at this rotation the total number of independent moduli is reduced to 12. The value of C'_{ij} and Young's and shear moduli are given in table 6,, for X' and Z' rotated to the principal axes of the spontaneous strain.

3.3. Accuracy of C_{ij} determination as indicated by elastic symmetry of rotated axes

As an indication of the error limits on the C_{ij} determination it is of interest to note the internal consistency of the extremal values of the critical angles θ, and their relation to the (602) plane domain-wall orientation as determined by Tsunekawa and Takei (1978) for monoclinic $LaNbO_4$ at 300 K. From standard calculations of interplanar angles, the (602) crystal plane is calculated to be 161° from the $(\bar{1}00)$ plane normal, using $a_0 = 5.567$ Å and $c_0 = 5.204$ Å. The determinatijon of θ_1 from the minimum value of C'_{55} or

Table 5. Elastic moduli of monoclinic $LaNbO_4$ for X rotated 75 and 165° from X, in (010) plane (X in domain wall) (units of 10^2 GPa).

$C'_{11} = C'_{33} = 2.35$	$C'_{55} = 0.03$
$C'_{22} = C'_{22} = 1.77$	$C'_{44} = C'_{66} = 0.49$
$C'_{12} = 0.60$	$C'_{15} = C'_{35} = 0.18$
$C'_{23} = 0.73$	$C'_{25} = 0.05$
$C'_{13} = 1.76$	$C'_{46} = 0.06$
$E_{X'} = E_{Z'} = 1/S'_{11} = 1/S'_{33} = 0.63$	
$G_{X'Z'} = 1/S'_{55} = 0.007$	

Table 6. Elastic moduli of monoclinic $LaNbO_4$ for X' rotated 30° from X in (010) plane (X' and Z' collinear with principal axes of spontaneous strain) (units of 10^2 GPa).

$C'_{11} = 2.45$	$C'_{55} = 0.30$
$C'_{33} = 1.73$	$C'_{44} = 0.39$
$C'_{22} = C_{22} = 1.77$	$C'_{66} = 0.60$
$C'_{12} = 0.90$	$C'_{15} = C'_{35} = 0$
$C'_{23} = 0.44$	$C'_{25} = 0.23$
$C'_{13} = 2.03$	$C'_{46} = 0.08$
$E_{33} = 1/S'_{33} = 0.023$	
$E_{11} = 1/S'_{11} = 0.04$	
$G_{X'Z'} = 1/S'_{55} = 0.250$	

maximum S'_{55} is $\theta_1 = 164 \pm 1°$, where

$$S'_{55} = 4l^2n^2(S_{11} - 2S_{13} + S_{33}) + 4ln(n^2 - l^2)(S_{15} - S_{35}) + (l^2 - n^2)^2 S_{55} \tag{5}$$

and l and n are the cosines of the angle between X' and X and between X' and Z, respectively, and

$$S_{ij} = \frac{\pm|C|_{ij}}{|C|} = \frac{\text{cofactor of } C_{ij}}{\text{determinant of } C_{ij} \text{ matrix}}$$

involves all of the measured C_{ij}. The reasonably good agreement between the observed domain-wall direction and the calculated θ_1 indicates that the errors of C_{ij} values determined by the best-fit method are of the order of 1%. This conclusion is enhanced when the agreement in θ_1 for $S'_{11} = S'_{33}$ (figure 10) and $C'_{44} = C'_{66}$ (figure 13) is analysed. The condition for this agreement is as follows:

$$\frac{\cos^2\theta_1 - \sin^2\theta_1}{2\cos\theta_1 \sin\theta_1} = \frac{2C_{46}}{C_{66} - C_{44}} = \frac{S_{15} + S_{35}}{S_{33} - S_{11}}. \tag{6}$$

From the values of the C_{ij} and S_{ij} for $LaNbO_4$ given in table 2, then

$$2C_{46}/(C_{66} - C_{44}) = 1.838 \qquad \text{gives} \qquad \theta_1 = 165.7° \tag{7}$$

and if we assume a 1% possible error in each modulus, the possible error in θ_1 is 1°; also

$$(S_{15} + S_{35})/(S_{33} - S_{11}) = 1.736 \qquad \text{gives} \qquad \theta_1 = 165.0° \tag{8}$$

and for an error of 2% in each S_{ij}, the θ_1 possible error is 3°. Thus the self-consistency between equations (7) and (8) is further evidence of reasonably high accuracy of the data.

4. Summary

(a) Measurements of acoustic wave velocities by ultrasonic and Brillouin light scattering techniques have enabled the determination of the single-crystal elastic moduli in the monoclinic ferroelastic phase of $LaNbO_4$ at 300 K (Nevitt *et al* 1986). The analysis of the data shows that the soft transverse mode propagated in the (010) plane, ρV_T^2, occurs for the two directions within 3° of the domain-wall directions, which are also the soft acoustic mode directions reported by Hara *et al* (1985) for the paraelastic tetragonal phase at T_0, the transformation temperature.

(b) By calculation of the elastic stiffness moduli, C'_{ij}, and elastic compliance moduli, S'_{ij}, as a function of rotation of the X and Z axial vectors about the $\langle 010 \rangle$ or Y axis in the monoclinic phase, it is shown that the elastic and acoustic symmetry along the domain-wall direction is uniquely pseudo-tetragonal in that the number of independent C'_{ij} is reduced to 10 as opposed to 13 for general monoclinic symmetry. This similarity to the tetragonal-phase acoustic properties arises from the parallelism of the domain-wall direction below T_0 to the direction of pure transverse mode of propagation above T_0. Thus the domain-wall atomic structure is the least distorted by the spontaneous shear strains that lead to the monoclinic symmetry. This direction in the monoclinic (010) plane has a very small C'_{55} shear modulus but a very high Young's modulus. A small internal tensile stress along this direction will produce only a very small collinear tensile strain and also only a small cross-coupled shear of the (010) plane.

(c) On the other hand, the direction in the (010) plane at 45° to the domain-wall direction has the maximum shear modulus, C'_{55}, the minimum Young's moduli and zero cross-coupling moduli, S'_{15} and S'_{35}. This is the direction collinear with the principal axis of the spontaneous strain that occurs at T_0. Thus a tensile or compressive stress along this direction will produce larger collinear tensile strains but there will be no coupled shear distortion. This result is the physical analogue to the analysis of David (1983) which states that the ferroelastic phase is most stable with respect to external tensile stress when the latter is collinear with the principal axes of the spontaneous strain.

(d) It is shown that the ultrasonic data of Avakyants *et al* (1982) for the C_{ij} of monoclinic $BiVO_4$ at 300 K are also consistent with the angle in the (010) plane of the soft transverse acoustic mode determined by several other Brillouin scattering studies above and below T_0. It is also shown that the correspondence of the rotated elastic moduli, C'_{ij} and S'_{ij}, with the domain-wall directions and the directions of the principal axes of spontaneous strain are qualitatively similar to what is observed in $LaNbO_4$. The principal differences in the results for $BiVO_4$ and $LaNbO_4$ are that the variations of ρV_T^2 and the C'_{ij} with rotation about the Y axes are almost an order of magnitude more severe in $LaNbO_4$. $BiVO_4$ has no near-zero soft acoustic mode at 300 K.

(e) Although the correspondence between the wave velocity measurements and the directions of wave propagation may have been in error, for one or more modes, because of the deviations of ultrasonic energy flux from propagation direction in the small $LaNbO_4$ crystals, the internal consistency of the measurements of critical angles for the domain-wall directions from different C_{ij} and S_{ij} combinations is remarkably good and indicates that basic C_{ij} determination is accurate to within 1%.

Acknowledgments

The author is indebted to Drs M V Nevitt, S K Chan and M H Grimsditch for permission to cite velocity data for $LaNbO_4$ before publication, and for technical assistance in preparing the manuscript of this paper and to the Hawaii Institute of Geophysics for use of computer facilities.

References

Avakyants L P, Antonenko A M, Dudnik E F, Kiseler D F, Mnushkina I E and Firsova M M 1982 *Sov. Phys.–Solid State* **24** 1411–12

Benyuan G, Copic M and Cummins H Z 1981 *Phys. Rev.* B **24** 4098–100
Cady W B 1946 *Piezoelectricity* (New York: McGraw Hill)
Cho M, Yagi T, Fujii T, Sawada A and Ishibashi Y 1982 *J. Phys. Soc. Japan* **51** 2914–19
David W I F 1983 *J. Phys. C: Solid State Phys.* **16** 5119–26
David W I F and Wood I G 1983 *J. Phys. C: Solid State Phys.* **16** 5127–48
Farley J M and Saunders G A 1972 *J. Phys. C: Solid State Phys.* **5** 3021–31
Farley J M, Saunders G A and Chung D Y 1973 *J. Phys. C: Solid State Phys.* **6** 2010–19
—— 1975 *J. Phys. C: Solid State Phys.* **8** 780–6
Hara K, Sakar A, Tsunekawa S, Sawada A, Ishibashi Y and Yagi T 1985 *J. Phys. Soc. Japan* **54** 168–72
Nevitt M V, Chan S K, Grimsditch M H and Fisher E S 1986 *Mater. Res. Soc. Materials Characterization Symp. (Palo Alto, CA)*
Tokumoto H and Unoki H 1983 *Phys. Rev.* B **27** 3748–61
Tsunekawa S and Takei H 1978 *Phys. Status Solidi* a **50** 695–702
Zalkin A and Templeton D H 1964 *J. Chem. Phys.* **40** 501–4